RESEARCH ARTICLE | FEBRUARY 18 2020

Mechanical design of interaction chamber for the ELIADE array at ELI-NP

Mihaela Violeta Munteanu ; Mircea Mihălcică ; Călin Itu ; Sorin Vlase; Maria Luminita Scutaru

AIP Advances 10, 025129 (2020)
https://doi.org/10.1063/1.5129317

Mechanical design of interaction chamber for the ELIADE array at ELI-NP

Cite as: AIP Advances 10, 025129 (2020); doi: 10.1063/1.5129317
Submitted: 30 September 2019 • Accepted: 25 January 2020 •
Published Online: 18 February 2020

Mihaela Violeta Munteanu,[a] Mircea Mihălcică,[b] Călin Itu,[a] Sorin Vlase,[a] and Maria Luminita Scutaru[a]

AFFILIATIONS

Department of Mechanical Engineering, Faculty of Mechanical Engineering, Transilvania University of Braşov, B-dul Eroilor 29, 500036 Braşov, Romania

[a]Electronic addresses: v.munteanu@unitbv.ro; calinitu@unitbv.ro; svlase@unitbv.ro; and lscutaru@unitbv.ro
[b]Author to whom correspondence should be addressed: mihalcica.mircea@unitbv.ro

ABSTRACT

This paper presents the analysis of the vibration of the interaction chamber (IC), a medium vacuum chamber, that uses linear actuators controlled on the basis of complex signals acquired from the IC and its surrounding space. This research mainly focuses on the kinematic precision assured by the mechanical system represented by the IC with component parts. The performance obtained by the quadrature acting system for the sample holder will be compared with the error introduced. The software implements two loops: the image acquisition from the digital camera and the detection of the target for the X–Y linear stage. Considering the vibration of the structure, the geometry of the whole system, the kinematics, and the dynamic model are detailed; the hardware's influence, in conjunction with the corresponding firmware of the tracking installation, is analyzed with regard to positioning precision and dynamics. For the IC, the transmissibility from the ground to the target (which is an important measure for the correct functioning of the system) was determined. As a result, it is necessary to re-design the target's lever in order to reduce the vibrations during the experiments.

I. INTRODUCTION

The ELI-NP Array of DEtectors (ELIADE) is one of the experimental setups being built at the ELI-NP (Extreme Light Infrastructure-Nuclear Physics).[1] The ELICAM GAMMA team, comprising researchers from the National Institute of Physics and Transilvania University of Brasov, investigated the possibilities of using appropriate solutions for good control of the mechanical system built for the conversion of a gamma "image" into a visible image using adequate scintillators and for positioning the target inside the gamma beam. In this paper, we present only the analysis of the vibration of the interaction chamber (IC)—the mechanics, optics, electronics, and control require further research.

The reaction between the straight brilliant gamma beam and different types of matter (the target to be touched by the beam) takes place in the interaction chamber (IC). The main role of the interaction chamber (see Fig. 1) is to maintain the samples exactly in the middle of the gamma beam. A system of detectors for tracking the nuclear reaction products is placed around the IC. These are positioned with high relative precision related to the IC and fixed space. Thus, the tracking of the brilliant gamma beam is not only important but also necessary to know, with high precision, the relative position between the sample holder placed inside the IC and the ELIADE detectors. The IC must be maintained, with precision, in the center of the straight gamma beam for a very long period of time (even for weeks). The precision required for an experiment with gamma beam rays is determined by the size of the target. For example, if we have enough target material for an experiment so that we can choose a target of any size, then the precision is not very important. However, if we have very small quantity of the target material, then the precision becomes very important. The aim was to reach a precision of about 2 μm, which would be satisfactory for most experiments. The gamma beam produced by the ELI-NP high power laser system is not rigorously constant and presents slight variations in the intensity and the direction.[2–4]

The device represents a source of discovery of new subelementary particles and related phenomena. The IC is a medium

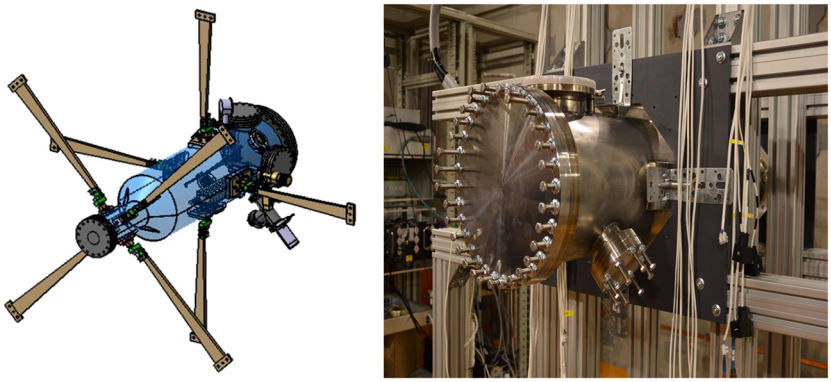

FIG. 1. The interaction chamber: (left) sketch and (right) physical device.

vacuum chamber that uses linear actuators controlled on the basis of complex signals acquired from the IC and its surrounding space.[5–7]

An alignment system is attached to the IC for tracking the fluctuations of the beam in real-time and also for maintaining the target reported on the gamma beam with very strict limits. Figure 2 illustrates how the detectors are positioned relative to the IC and the detection system that allows tracking of the variation in the direction of the brilliant gamma beam in real-time. The IC is kept in a fixed position relative to the detectors and fixed space. The alignment system acts only on the sample holder by moving it inside the IC. In order to avoid reactivity artifacts, the IC permits a medium vacuum. The tracking system is a complex one and includes four main components:

1. the mechanical sub-system necessary to support the linear stages (actuators endowed with step by step motors) that assure the movement of the sample holder in a plane on the X- and Y-axis;
2. the optical system that converts the gamma beam image on a scientific CMOS (sCMOS) digital camera;
3. the electronic sub-system that implements the image acquisition system and also the driver sub-systems that control the positions of the linear stage; these linear stages are used to move the sample holder on the X- and Y-axis; and
4. the software that implements the main tracking functionalities of the sample holder.

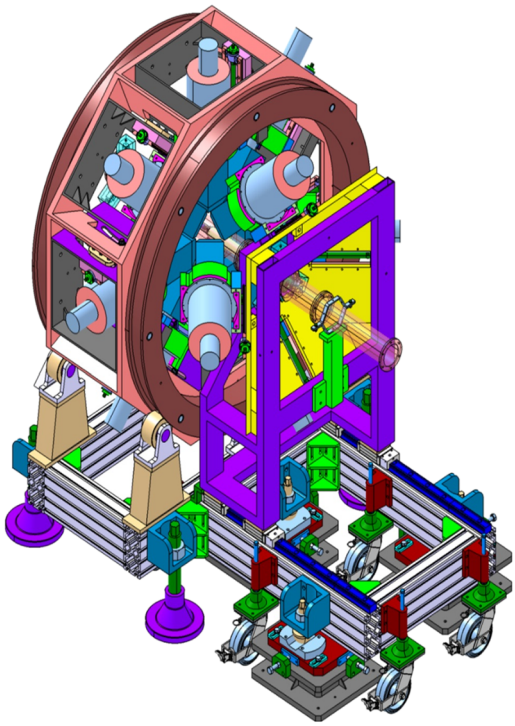

FIG. 2. The interaction chamber with the ELIADE sensor sub-system.

Before the system's implementation, the following scientific and technological challenges are raised:

- to assure a high-fidelity detection and conversion of a gamma image into a visible image;
- to accurately take into consideration all dependencies between test bench elements, geometric shape, and distances between system elements, such as relative positions between the interaction chamber and ELIADE detectors;
- to put in evidence and dynamically correct the mechanical system's structure variation due to vibrations and temperature variation (dilatations and contractions);
- to avoid the influence of high energy photons on the electronic tracking elements; and
- to improve the methodologies for the identification of dynamic reference points revealed on the image generated by the interaction between the brilliant gamma beam, samples, and their motorized holder placed inside the interaction chamber.

Until now, fundamental research aspects that must be clarified during long term experiments remain important, such as the complexity and the insufficiently known reactions between the brilliant gamma beam and the matter used as samples (nuclear reactions) and the fluorescence of irradiated objects. In addition, some technical aspects such as accurate target landscape image acquisition and serial precision in positioning offered by the linear stages

(controlled on the basis of the real acquisition and image feature detection of targets and their holders placed inside the interaction chamber) are not sufficiently known and need innovative solutions.

This paper mainly focuses on the kinematic precision assured by the mechanical system represented by the interaction chamber with its component parts. For this, vibration analysis of the system using the finite element method (FEM) is necessary and represents the main purpose of this paper. The performance obtained by the quadrature acting system for the sample holder will be compared with the error introduced considering the vibration of the structure. Some relevant details that permit the understanding of the solution and its conjunction with the determination and performance of positioning technology are presented. The geometry of the whole system, the kinematics, and the dynamic models are detailed; the hardware's influence, in conjunction with the corresponding firmware of the tracking installation, is analyzed with regard to positioning precision and dynamics. All these factors are important to obtain a high accuracy of measurement.

The static and dynamic dependability between the position of the interaction chamber, the position of the sample support therein, and the relative movement introduced by the tracking system of the directional variations of the gamma beam are emphasized.

The software developed for the compensation of errors and for the adjustment of overall results done by the test bench during long-term experiments is improved, and the testing methodology and experimental setup are explained.

Finally, the conclusions clearly emphasize the future steps toward the complete utilization of the infrastructure generated by the 16ELI-2016 project.

A synthetic image puts in evidence the main tracking brilliant gamma beam system:

- a mechanical subsystem used as support for all the other components;
- an optical system, necessary to convert the high energy beam projected to an image plane in a visible image, which in turn is projected to the high resolution, high sensitivity, and exceptional precision sCMOS image sensor;
- an electronic system, necessary for image acquisition processing and controlling the sample holder position inside the interaction chamber; and
- the embedded software designed to implement all the component functionalities and also the overall programs.

II. A SHORT DESCRIPTION OF THE ELI-GAMMA SYSTEM

The ELI-GAMMA electronic system is placed on the experimental perimeter of the ELI laboratory. The main goal is to host different nuclear physics experiments. The samples are inserted into the interaction chamber and are held in the gamma beam path by a holder. The holder's shadow is projected on the scintillator's surface plane.[8] This will convert the projected image from the gamma spectrum to the visible spectrum, generating an image that will be transferred by the optical system in an image projected to the sCMOS camera.

The system acquires the image of the "shadow" made by the passage of the gamma beam through the interaction chamber in which the support of the tested samples is found. The shadow is determined by measuring the intensity of the radiation generated by the scintillator, whose image is projected using the optical system on the sCMOS image sensor. The scintillator converts the image from the gamma domain that is designed on it during operation into the visible domain. This "image" in the visible field is the result of the incidence of the gamma photons crossing the interaction chamber. The optical path of the gamma beam will be dependent on the components in the path of the gamma beam, namely, the walls of the interaction chamber and all the elements that are incident to the beam, including the sample support. Thus, a "fingerprint" appears (i.e., a characteristic image) because the attenuation factor will be dependent on the path in which the gamma photons propagate. This fingerprint is in the visible field, which will be captured by the sCMOS camera. These images are taken periodically, and the areas of equal illumination are detected (the same shade of gray, i.e., the same number of electrons generated on the sensor as a result of the projection of the converted image using the scintillator).

A point in the image is selected and its position is considered as a reference at the time of acquisition of the gamma incident beam. The system will try to maintain the same position relative to the point determined at the initial moment, regardless of the possible time variation of the direction of the incident gamma beam in the interaction chamber.

The precision with which it does this is the result of two factors:

- the resolution of the sCMOS camera (2048 × 2048 pixels), the optical system of projection of the images of the scintillator, and the scintillator itself, and the accuracy in positioning given by the actuators that, according to the tracking algorithm of the point, will be commanded to maintain the reference point in the same position with the initial one;
- the precision of the actuators (stepper motors equipped with nut mechanism—trolley) in positioning is better than 2–5 μm, meaning it is better than 3–4 increments (steps) corresponding to the stepper actuator (given in the technical specification by the engine manufacturer, an increase is made with a precision of 1.23 μm).

A. The interaction chamber

In the laboratory, an sCMOS camera is used: it is a scientific camera with excellent features such as signal to noise ratio (SNR), adaptable sensitivity, and high resolution (2048 × 2048 pixels). This permits complex triggering modes. A precision acting system functioning in vacuum was chosen (Figs. 3 and 4) to move the sample holder. The link between the camera and the computer is implemented by a fast USB 3.0 interface.

The interaction chamber is fixed on two planes where two actuators assure the movement of the interaction chamber on the gamma beam's direction. The kinematics of the action system was designed, simulated, and experimentally validated. In order to have an initial "reference position," a laser visible beam independent alignment

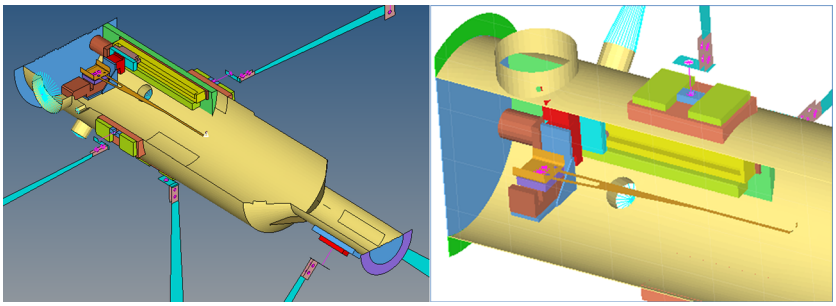

FIG. 3. Inside of the interaction chamber (sections).

system was used. This will assure the raw alignment of the interaction chamber, and the designed system will take this point as a reference for all future alignment commands done on actuators. We assume that the image of the sample holder and the other interaction chamber elements will generate a characteristic shadow on the scintillator and this will be captured through the optical system by the sCMOS digital camera. These patterns are displayed on computer monitors, and the operator can interactively indicate the object used as a reference. After the first step, when a potential mark is identified, the system will automatically calculate the alignment error and will adequately command the motors to minimize it. The software implements two loops: (i) the image acquisition from the digital camera and (ii) based on image processing, the detection of the target for the X–Y linear stage will be activated with the updated target value (see Fig. 5). In this stage, the computer will transmit the new reference values for Brushless DC (BLDC) actuators isosynchronously with the image acquisition. The maximum sampling rate can slightly vary during the functioning of the tracking system, as a result of processes that run on the computer. The operating system used is Windows 10 (does not guarantee an exact time of execution for each thread). The experimental results show that the whole control loop has a period of less than 100 ms (10 sps), which is in accordance with the slight variations of the brilliant gamma beam's direction.

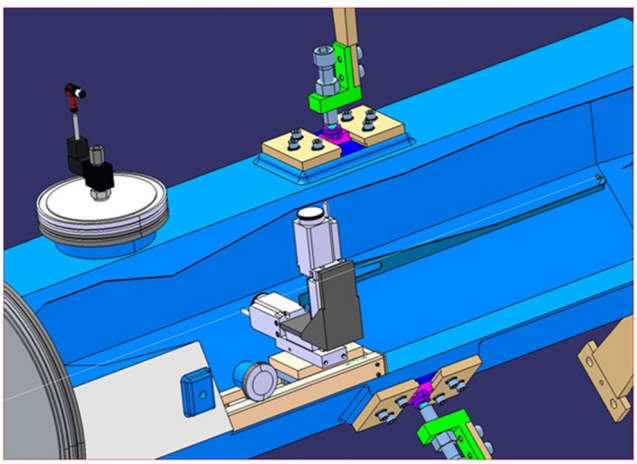

FIG. 4. The actuators' system and the lever with the target.

The image captured by the digital camera will be synchronized as an acquisition with the main signal provided by the ELI system in order to avoid the errors related to the sampling period in the image acquisition. The algorithm periodically commands the acquisition of images from the digital camera or uses the synchronization signal for that. The successive images are compared in order to detect the eventual relative sliding of the beam. In Fig. 5, the detailed algorithm of the ELI-GAMMA system is shown. The material from which the camera and the other devices are made is chosen according to the recommendations in Refs. 9–11.

B. The optics of the tracking system

While not so important in our future considerations, a short description of this system is needed. The scintillator is placed near the interaction chamber's wall, perpendicular to the gamma beam direction, which converts the incident gamma image into a visible fluorescence image in the scintillator's plane. A $Bi_{12}GeO_2$ (BGO) scintillator, compatible with the photon energy used for this application, is used. Special attention was paid for the simulation of the interaction between the gamma beam and scintillator material. As shown in Fig. 2, the main tracking brilliant gamma beam detection system is mounted on the IC. The sample holder's shadow is converted into a visible fluorescence image in the scintillator's plane.

Slight variations in the direction of emission of the source, in correlation with the relative movement vs the fixed space of the interaction chamber, can cause detectable errors. These errors can affect the accuracy of the relative position of the target (sample) used in the ELI system and located in the interaction chamber (Fig. 6). As it can be easily seen in Fig. 6, because the ELIADE detectors have a fictitious position, as is the gamma source, the slight variations in its direction of emission in correlation with the relative movement relative to the fixed space of the interaction chamber cause relative detectable errors, which may affect the accuracy of the relative position of the target (sample) used in the ELI system and located in the interaction room.

III. FE ANALYSIS OF THE FREE VIBRATION OF THE IC

Using the Lagrangian and applying the Lagrange equation, we obtain[12]

$$\frac{d}{dt}\left\{\frac{\partial L}{\partial \dot{\delta}_e}\right\} - \left\{\frac{\partial L}{\partial \delta_e}\right\} = 0, \quad (1)$$

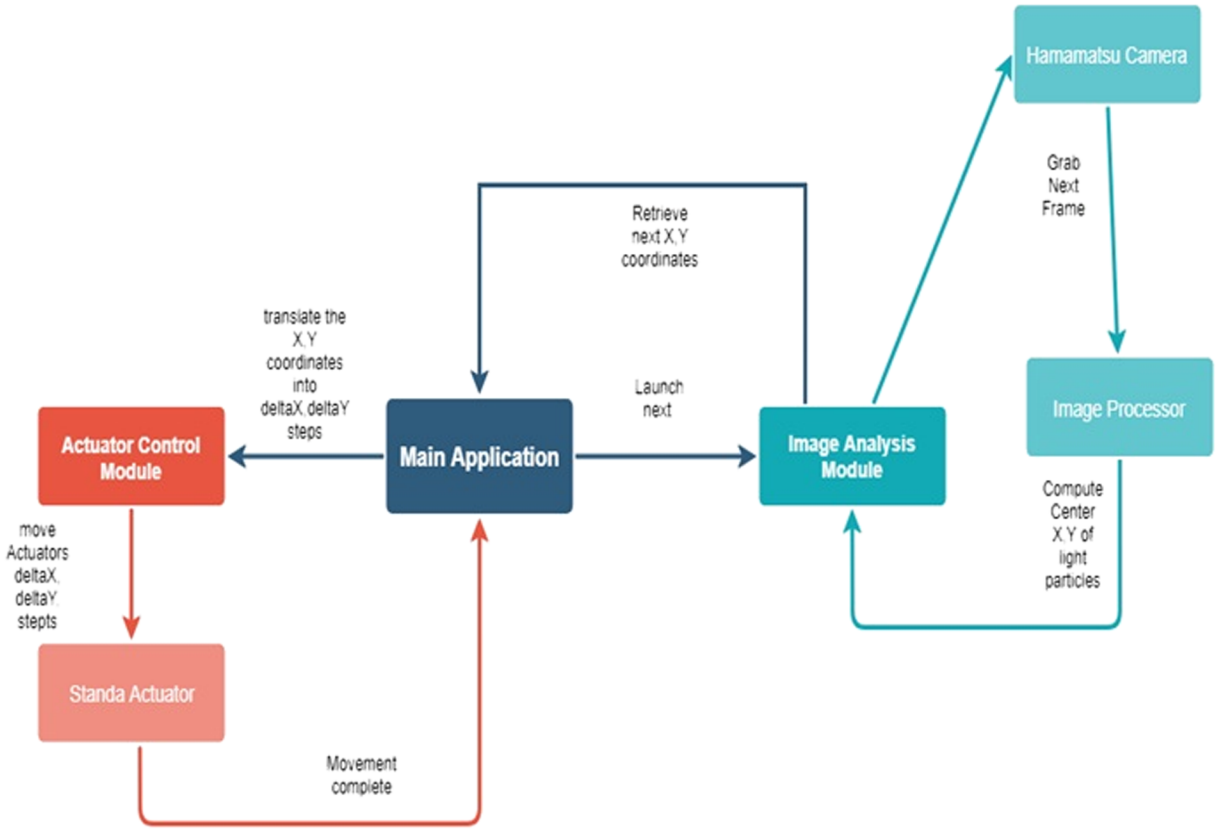

FIG. 5. Detailed image of the ELI-GAMMA beam tracking system.

where the Lagrangian has the form[13–15]

$$L = E_c - E_p + W + W^c. \tag{2}$$

The kinetic energy due to the translation is, in this case,[16–18]

$$E_c = \frac{1}{2}\int_0^L \rho \dot{X}'_k \dot{X}'_k dx_1 dx_2 dx_3, \tag{3}$$

where $\dot{X}'_k$ represents the velocities of the current point of the rigid, ρ is the density function, and x_k are the coordinates of a current point. The equations of motion shall be obtained in the local coordinates system. The potential energy (internal work) is[19–23]

$$E_p = \frac{1}{2}\int_V \sigma_{ij}\varepsilon_{ij} dV, \tag{4}$$

where σ_{ij} represents the stress tensor and ε_{ij} represents the strain tensor.

The Hooke law can be written as follows:

$$\sigma_{ij} = D_{ik}\varepsilon_{kj}. \tag{5}$$

After some calculus, the motion equations are obtained in the form[24,25]

$$m_{e,ij}\ddot{\delta}_{eL,j} + 2c^{\omega}_{e,ij}\dot{\delta}_{eL,j} + \left(k_{e,ij} + k^{\varepsilon}_{e,ij} + k^{\omega^2}_{e,ij}\right)\delta_{eL,j} = q_{e,i} + q^{*}_{e,i} - q^{\varepsilon}_{e,i} - q^{\omega^2}_{e,i} - m^{0}_{e,ij}\ddot{x}_{j0}. \tag{6}$$

The matrix coefficients are determined by choosing the shape functions and the nodal coordinates of a point. Following the well-known procedures of referring the motion equations of the finite element to the global reference system and assembling all these

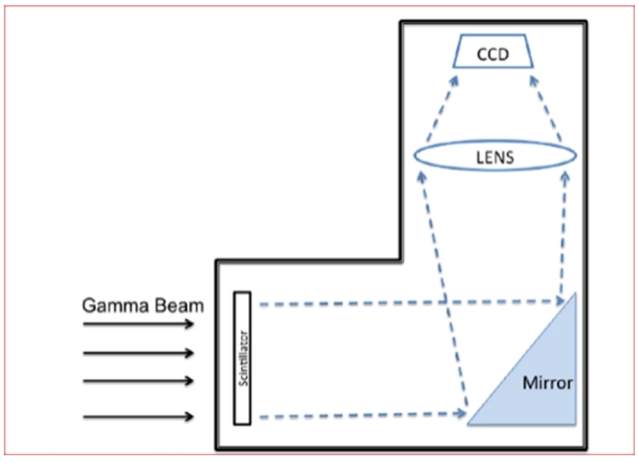

FIG. 6. The relative position of the camera vs the gamma beam.

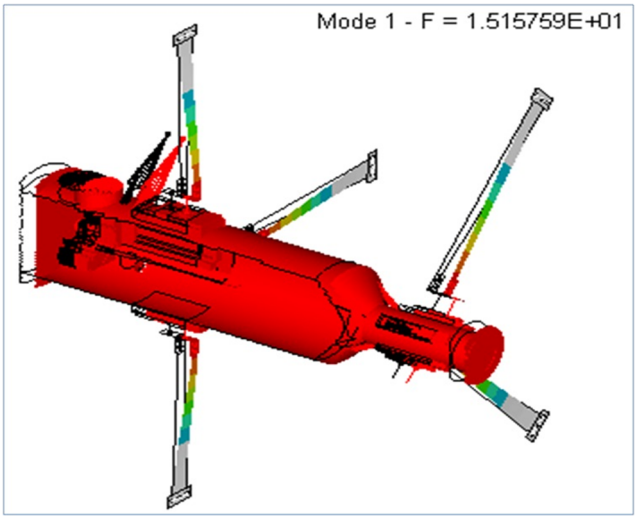

FIG. 7. First eigenvalue (Hz) and its corresponding eigenmode.

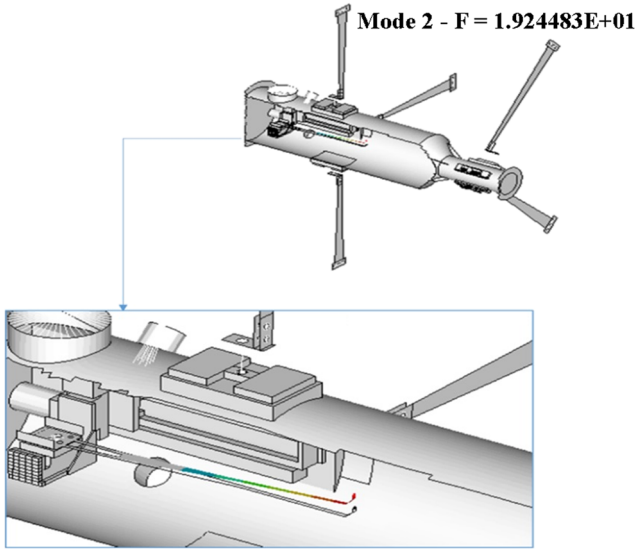

FIG. 8. Second eigenvalue (Hz) and its corresponding eigenmode.

equations, ultimately the motion equations for the entire structure are obtained. This set of equations is then used in the dynamic analysis.[26–29]

The FE analysis was conducted in two steps. First, the eigenvalues and eigenvectors are determined in order to identify the main eigenmode of vibration of the system. The transmissibility of the displacement from the ground and the one from the body of the interaction chamber to the target is determined in the second step. These become important due to the fact that the electric engine brings a load that can cause vibration. It is difficult to determine the vibration determined by the operation of actuators by calculus, and it is necessary to make experimental tests to see the values of the amplitude. Once these values and the transmissibility of the system (determined using FEM) are known, one can determine the deviation of the target from the ideal position due to vibrations. The position of the

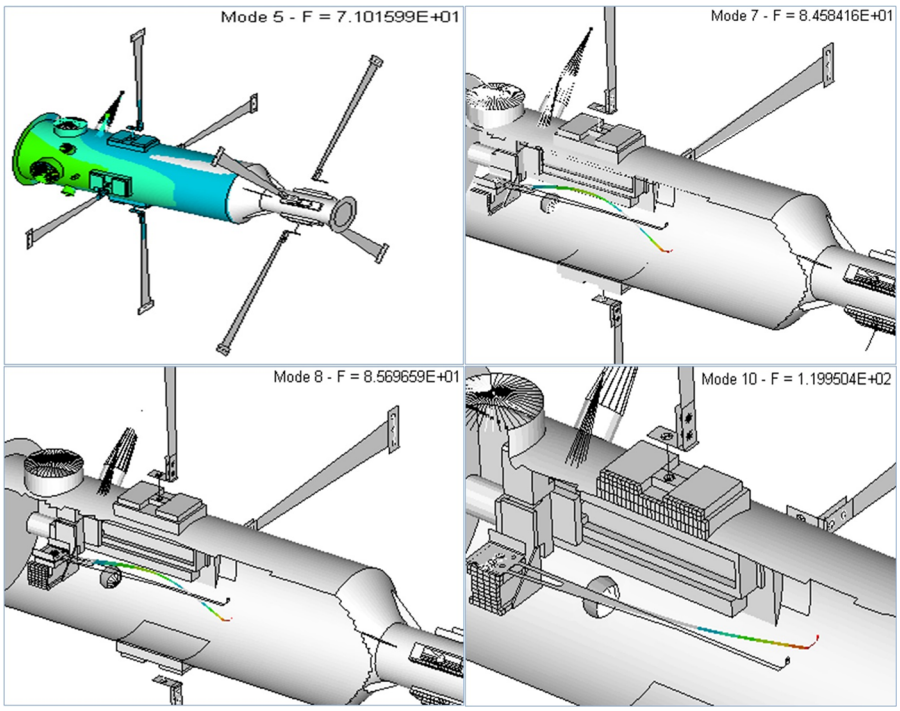

FIG. 9. Eigenvalues and eigenmodes 5, 7, 8, and 10 (Hz).

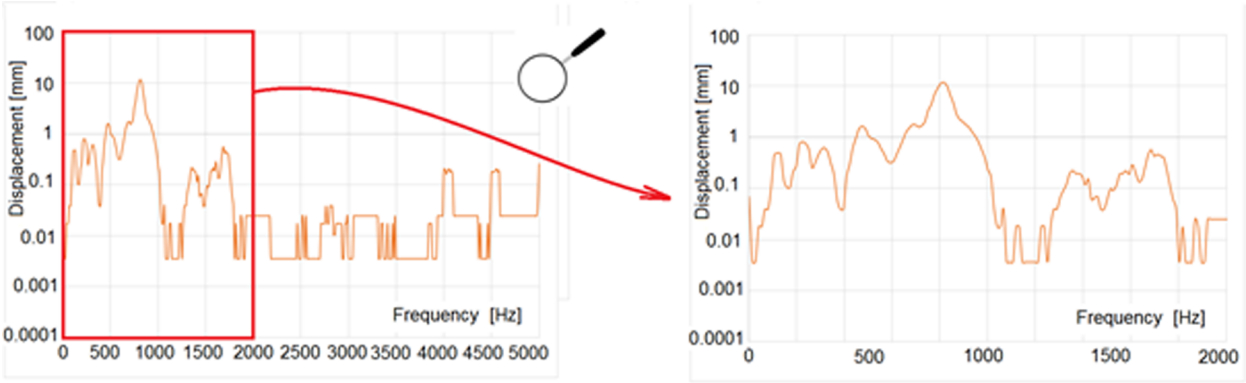

FIG. 10. The transmissibility of the displacement of the ground.

gamma beam ray is considered to be fixed during the experiment (this is provided by the system built at ELI-NP, Bucharest).

The precision provided by the mechanical system is 2 μm, which is considered to be sufficient for most experiments. The problem that arises is that of the vibrations induced by the actuating motors as well as by other equipment in the complex system that hosts the interaction chamber. For an experiment that takes place over a long period, the existence of these vibrations is insignificant. The problem arises when it is necessary to carry out an experiment in which the target of the material to be tested is small and the exposure time is also very short (seconds). This type of experiment requires vibration calculations (ideally, we should know the amplitudes of the forced vibrations and they should be smaller than a quarter of the target's diameter).

In the following, we present some values of eigenfrequencies and corresponding eigenmodes. The first mode of vibration shows a dilatation for the whole body of the interaction chamber (see Fig. 7). The second eigenmode depicts the vibration of the lever with the target, an interesting finding of our study (see Fig. 8).

The eigenmodes 7, 8, and 10 (Fig. 9) present the eigenvibrations of the lever. This means that, for an excitation frequency near this calculated eigenfrequency, it is possible that the amplitude of the lever increases in such a way that it brings very large errors. In practice, all these eigenvalues must be avoided.

In order to determine the transmissibility of the displacement, we imposed a uniform displacement of the lever holding area in a vertical direction and we determined by calculation, using the finite element method, the vertical displacement of the target. The amplification factor is shown in Fig. 10. It can be observed that, for some excitation frequencies, the target amplitude can be 13 times greater than the displacement of the support point (due to the vibrations induced by the electric motors). The problem of the vibrations can be solved in two ways: either increasing the rigidity of the lever in order to change its elastic properties and decrease the transmissibility and/or introducing a damping system for the same purpose. The proposed solution is to change the lever shape with a plate with a ribbed surface. This solution is being studied right now. Changing the material may be risky because it is not known how different materials behave at a gamma-ray beam of such magnitude.

IV. THE TESTING METHODOLOGY AND EXPERIMENTAL SETUP

Two different elements may cause the target to be removed from the range of the gamma-ray: the vibration caused by the movement of the actuators and the positioning errors caused by the joints in the moving elements of the positioning system. The measurement must determine the errors due to the joints and, on the other hand, the displacement of the holding area.

The methodology for testing the linear stages, endowed with step motors, is adequate for the chosen solution. Specifically, open-loop solutions were adopted, which are more precise if all the potential errors are detected and corrected or compensated. The linear stages are adapted to function on vacuum conditions. We have designed a methodology that can highlight the positioning error produced by the linear stage. It is necessary to know that the step of the motor is 1.25 μm in the open-loop regime. The driver used to control the motor allows the determination of the step done by the minor loop procedure that is based on current variation recognition when the motor executes a step. A test bench was designed, and this includes the computer used for the control of the linear stage, the test bench that assures the exact relative positioning of the linear stage, the linear digital sensor, and the holder for the weight used as a supplementary load. The proportional integral differential (PID) regulator of the linear stage was maintained with its default parameters. The summary of the experimental testing system is described in Fig. 11, and the components of the experimental testing system are as follows:

- STANDA 8MT173V-30-VSS42 precision motorized compact translation stage,
- STANDA 8SMC5-USB stepper and DC motor controller,
- data acquisition system for the Heidenthain-Metro MT 2500 length gauge,
- Heidenhain-Metro MT 2500 length gauge, and
- mechanical stand.

The equipment was set up on a heavy table, on a cement floor with rubber dampers, in order to minimize as much as possible any unwanted mechanical vibrations. The actuator was fitted to the

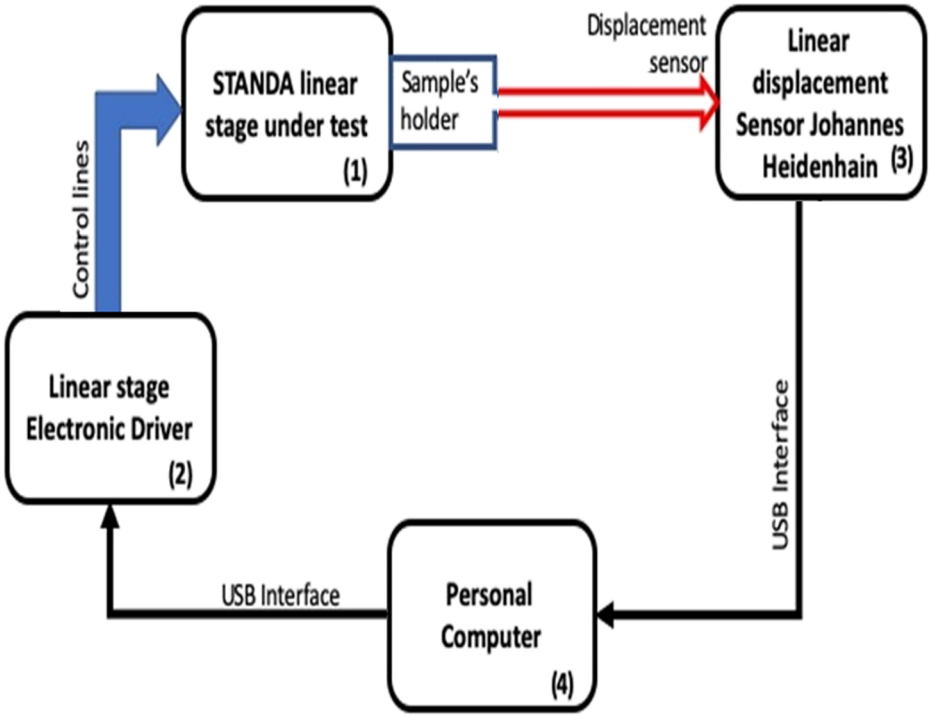

FIG. 11. Block diagram of the testing system.

mechanical stand using a number of bolts, and the length gauge was held in place using a magnetic fitting—this held it firmly in position, but also allowed for easy repositioning if needed.

After fitting the actuator, the length gauge was aligned properly to it—the sensor uses a mechanical plunger in order to measure linear motion; this plunger was aligned parallel to the direction of extension of the mechanical arm the actuator controls, thus removing any distance correlation issues. The actuator was connected to the stepper and DC motor controller, which, in turn, was connected to a laptop, which ran the software for controlling the position of the actuator's extension arm. The sensor was connected to a data acquisition system (DAQ) through a serial port. The DAQ was connected to the laptop in order to store and process the data. The end of the length gauge plunger was put in contact with the tip of the extension arm.

After analyzing the experimental results, it can be observed that the errors due to the joints are less than 2 μm, while the amplitude of the vibrations of the holding system is less than 60 μm. This shows that it is important to redesign the lever in order to decrease the transmissibility of the displacements to the target. It is possible for the target to come out of the gamma-ray. It is true that, for most experiments, the target may be sized so large that there is no problem in reaching it by the gamma-ray beam. However, there may be an experiment where the target is of extremely small size and should, therefore, be sized to meet these requirements.

V. CONCLUSIONS

In this paper, a study concerning the vibration of the reaction chamber of the ELIADE array is made. The transmissibility from the ground to the reaction chamber and to the target is an important measure for the correct functioning of the system. The foundation and the ground of the laboratory are built in order to provide good isolation to vibrations. However, predictable and unpredictable excitations of the reaction chamber may occur. Inside the interaction chamber, there are three actuators that allow the target to move to the main flux of the gamma-ray beam. These actuators (if they act) induce vibration in the whole system. If the excitation frequency is close to the resonance frequency of the fixing mechanism, it is possible to have an amplification of the vibrations induced by the motors. The main purpose of this work is to help properly design the system considering the action of vibrations that may occur. The control of the position of the interaction chamber is assured by an original software implemented in two loops: (i) the image acquisition from the digital camera and (ii) the detection of the target for the X–Y linear stage. The computer will transmit the new reference values for Brushless DC (BLDC) actuators isosynchronously with the image acquisition. The maximum sampling rate can slightly vary during the functioning of the tracking system as a result of processes that run on the computer. The experimental results show that the whole control loop has a period of less than 100 ms (10 sps), which is in accordance with the slight variations of the brilliant gamma beam's direction. The results of the analysis show that a unit displacement of the ground can cause vibration with 13 times higher amplitude. This occurs for a frequency of about 790 Hz. Clearly, this frequency has to be avoided, and measurements have shown that motor-induced excitations are out of this range. However, the increase in the magnitude can occur at other frequencies (see Fig. 10). The target can suffer an important displacement, making it possible for the gamma beam to move out of the target. As a consequence, it may be necessary to resize this device with a fixing system in a way that the

transmissibility from the ground to the target decreases. The correct design of this interaction chamber is required. The material must be changed and a redesign of its shape must be made. The new shape must ensure lower transmissibility from the ground to the target. A proposed solution is to replace the lever shape of the target arm with a ribbed surface. It is difficult to replace the material from which the target arm is manufactured, as the material's response to the action of a gamma-ray of such power is unknown.

The following aspects were considered in the optical system tests:

- The duration of a complete control cycle (let us call it t), respectively, how long it takes to purchase, process, order, and execute the actuator command in the reference tracking process. In other words, we are interested in the maximum sampling frequency in control (1/t). The optical integration time is relatively long (0.04–0.05 s at least), and that is why a large aperture of the lens was desired along with a high sensitivity of the scintillator and sCMOS, i.e., measures were taken to minimize the complete sampling cycle of the system.
- To check what are the possible errors that the control system introduces when its mechanical load varies to identify the parameters of the purchased position regulator with the help of which we command the stepper actuators. For the moment, we have shown, with an optical laser in the visible, what in the future will represent the image in visible but converted from the gamma by the scintillator. At the time of writing this article, the gamma ray is not available yet, because the source is only now being built. As a result, some unknowns remain, both in the accuracy assessment and the possibility of instability phenomena.

ACKNOWLEDGMENTS

The authors would like to thank the Department of Mechanical Engineering of the Transilvania University of Brasov for providing laboratories and equipment. The authors acknowledge ELI-NP, Institute of Atomic Physics, Măgurele (Grant No. 16/2016), for financial support.

The authors declare no conflict of interest.

REFERENCES

[1] See www.eli-np.ro for more information about the Extreme Light Infrastructure Nuclear Physics project; accessed 1 June 2019.
[2] J. S. Bihalowicz, "The mini ELITPC: Reconstruction and identification of charged particles tracks during beam tests at IFIN-HH," in *2017 IEEE Proceedings of International Young Scientists Forum on Applied Physics and Engineering (YSF)* (IEEE, 2017), pp. 259–262.
[3] M. Cwiok *et al.*, "A TPC detector for studying photo-nuclear reactions at astrophysical energies with gamma-ray beams at ELI-NP," Acta Phys. Pol., B **49**(3), 509–514 (2018).
[4] C. Matei, D. Balabanski, D. M. Filipescu, and O. Tesileanu, "Photodisintegration reactions for nuclear astrophysics studies at ELI-NP," in *Nuclear Physics in Astrophysics Conference (NPA VII)* [J. Phys.: Conf. Ser. **940**, 012025 (2018)].
[5] O. Tesileanu *et al.*, "Charged particule detection at ELI-NP," Rom. Rep. Phys. **68**(Supplement 2), S699–S734 (2016).
[6] I. C. E. Turcu *et al.*, "High field physics and QED experiments at ELI-NP," Rom. Rep. Phys. **68**(Supplement 1), S145–S231 (2016).
[7] I. C. E. Turcu *et al.*, "Strong field physics and QED experiments with ELI-NP 2×10PW laser beams," AIP Conf. Proc. **1645**, 416–420 (2015).
[8] S. Vlase *et al.*, "Dynamic analysis of the reaction chamber for the ELIADE array," in *Acoustic and Vibration of Mechanical Structures (AVMS-2017)*, Springer Proceedings in Physics Vol. 198 (Springer, 2018), pp. 263–269.
[9] I. Negrean, "Advanced equations in analytical dynamics of systems," Acta Tech. Napocensis, Ser.: Appl. Math., Mech. Eng. **60**(IV), 503–514 (2017).
[10] M. I. A. Othman and M. Marin, "Effect of thermal loading due to laser pulse on thermoelastic porous medium under G-N theory," Results Phys. **7**, 3863–3872 (2017).
[11] H. Teodorescu-Draghicescu and S. Vlase, "Homogenization and averaging methods to predict elastic properties of pre-impregnated composite materials," Comput. Mater. Sci. **50**(4), 1310–1314 (2011).
[12] S. Vlase, "A method of eliminating Lagrangian-multipliers from the equation of motion of interconnected mechanical systems," J. Appl. Mech. **54**(1), 235–237 (1987).
[13] A. Midha, A. G. Erdman, and D. A. Frohrib, "Finite element approach to mathematical modeling of high-speed elastic linkages," Mech. Mach. Theory **13**(6), 603–618 (1978).
[14] P. K. Nath and A. Ghosh, "Steady-state response of mechanism with elastic links by finite element methods," Mech. Mach. Theory **15**, 199 (1980).
[15] B. S. Thompson and C. K. Sung, "A survey of finite element techniques for mechanism design," Mech. Mach. Theory **21**(4), 351–359 (1986).
[16] B. M. Bahgat and K. D. Willmert, "Finite element vibrational analysis of planar mechanisms," Mech. Mach. Theory **11**, 47 (1976).
[17] W. L. Cleghorn, E. G. Fenton, and K. B. Tabarrok, "Finite element analysis of high-speed flexible mechanisms," Mech. Mach. Theory **16**, 407 (1981).
[18] E. R. Christensen and S. W. Lee, "Nonlinear finite element modelling of the dynamics of unrestrained flexible structures," Comput. Struct. **23**(6), 819–829 (1986).
[19] A. G. Erdman, G. N. Sandor, and A. Oakberg, "A general method for kineto-elastodynamic analysis and synthesis of mechanisms," J. Eng. Ind. **94**(4), 1193 (1972).
[20] P. Fanghella, C. Galletti, and G. Torre, "An explicit independent-coordinate formulation for the equations of motion of flexible multibody systems," Mech. Mach. Theory **38**, 417–437 (2003).
[21] J. Gerstmayr and J. Schöberl, "A 3D finite element method for flexible multibody systems," Multibody Syst. Dyn. **15**(4), 305–320 (2006).
[22] M. Hassan, M. Marin, R. Ellahi, and S. Z. Alamri, "Exploration of convective heat transfer and flow characteristics synthesis by Cu–Ag/water hybrid-nanofluids," Heat Transfer Res. **49**(18), 1837–1848 (2018).
[23] S. Vlase, D. D. Scarlatescu, M. Marin, and A. Öchsner, "Finite element analysis of an elbow tube in concrete anchor used in water supply networks," Proc. Inst. Mech. Eng., Part L **234**, 3 (2019).
[24] S. Vlase, "Dynamical response of a multibody system with flexible elements with a general three dimensional motion," Rom. J. Phys. **57**(3-4), 676–693 (2012).
[25] S. Vlase, C. Danasel, M. L. Scutaru *et al.*, "Finite element analysis of a two-dimensional linear elastic systems with a plane rigid motion," Rom. J. Phys. **59**(5-6), 476–487 (2014).
[26] P. Boscariol, P. Gallina, A. Gasparetto, M. Giovagnoni, L. Scalera, and R. Vidoni, "Evolution of a dynamic model for flexible multibody systems," in *Advances in Italian Mechanism Science*, Proceedings of the First International Conference of IFToMM Italy (Springer, 2016), pp. 533–541.
[27] J. Mayo and J. Domínguez, "Geometrically non-linear formulation of flexible multibody systems in terms of beam elements: Geometric stiffness," Comput. Struct. **59**(6), 1039–1045 (1996).
[28] D. de Falco, E. Pennestri, and L. Vita, "An investigation of the influence of pseudoinverse matrix calculations on multibody dynamics by means of the Udwadia-Kalaba formulation," J. Aerosp. Eng. **22**(4), 365–372 (2009).
[29] A. A. Shabana, "Flexible multibody dynamics: Review of past and recent developments," Multibody Syst. Dyn. **1**, 189–222 (1997).